Published in final edited form as:
Annu Rev Anal Chem (Palo Alto Calif). 2009 ; 2: 409–433. doi:10.1146/annurev-anchem-060908-155146.

Analytical Chemistry of Nitric Oxide

Evan M. Hetrick and **Mark H. Schoenfisch**
Department of Chemistry, University of North Carolina at Chapel Hill, Chapel Hill, NC 27599

Mark H. Schoenfisch: schoenfisch@unc.edu

Abstract

Nitric oxide (NO) is the focus of intense research, owing primarily to its wide-ranging biological and physiological actions. A requirement for understanding its origin, activity, and regulation is the need for accurate and precise measurement techniques. Unfortunately, analytical assays for monitoring NO are challenged by NO's unique chemical and physical properties, including its reactivity, rapid diffusion, and short half-life. Moreover, NO concentrations may span pM to μM in physiological milieu, requiring techniques with wide dynamic response ranges. Despite such challenges, many analytical techniques have emerged for the detection of NO. Herein, we review the most common spectroscopic and electrochemical methods, with special focus on the fundamentals behind each technique and approaches that have been coupled with modern analytical measurement tools or exploited to create novel NO sensors.

Keywords

reactive nitrogen species; Griess assay; chemiluminescence; electron paramagnetic resonance spectroscopy; electrochemical sensors

1. INTRODUCTION

Prior to the late 1980s, nitric oxide (NO) was known primarily as an environmental pollutant. In 1987, Ignarro and Furchgott independently confirmed NO's role in mammalian physiology with the determination that NO was the long-elusive endothelium-derived relaxing factor (EDRF) responsible for vasodilation and blood pressure regulation (1,2). Since that discovery, a great deal of research has unraveled the multifaceted roles of NO. Indeed, NO plays key physiological roles in the cardiovascular (3) and nervous (4,5) systems, as an endogenously-produced antimicrobial agent (6), and as a signaling molecule capable of modulating cytokine production (7), the immune response (8), and wound healing (9). Endogenously, NO is produced by a class of heme-containing enzymes known as nitric oxide synthases (NOSs) (10,11). With respect to its pharmacological potential, several chemical NO donors have been developed to spontaneously generate NO (12,13), subsequently allowing for its further study.

The intense interest in NO research and the need to characterize chemical NO donors demands analytical techniques capable of accurately and precisely quantifying NO concentrations and rates of production. The unique chemical properties of NO make this a challenging task. For example, NO is highly reactive and rapidly scavenged by endogenous compounds including oxygen (O_2), heme proteins (e.g., hemoglobin), thiols (e.g., cysteine

Correspondence to: Mark H. Schoenfisch, schoenfisch@unc.edu.

DISCLOSURE STATEMENT
The authors are not aware of any biases that might be perceived as affecting the objectivity of this review.

residues, glutathione), and other free radicals (e.g., superoxide) (14–18). Nitric oxide's short-half life (on the order of seconds) thus complicates its detection. Moreover, NO's actions are mediated by a broad range of concentrations (from pM to μM, i.e., spanning ~6 orders of magnitude) (14,19), resulting in the need for techniques with wide linear response ranges. The rapid diffusion of NO and its transient nature further demand analytical methods with rapid response times for spatial detection (20).

Fortunately, the same chemical properties that make monitoring NO challenging also allow a broad range of analytical techniques to be employed for its detection. The primary methods for detecting NO include absorbance-, fluorescence-, and chemiluminescence-based approaches, electron paramagnetic resonance (EPR), and electrochemistry. This review will detail the fundamentals regarding these techniques, focusing on the applicable chemistry and analytical figures of merit including detection limit, linear range, response time, and selectivity for NO over common interferents. Special attention is given to newly-developed assays and approaches for which NO detection techniques have been either coupled with modern analytical measurement tools (e.g., HPLC) or exploited to create novel analytical sensors. Examples are chosen to illustrate both standard and new applications of each technique. The majority of this review focuses on spectroscopic and electrochemical NO detection methods, and a summary of each detection technique discussed is presented in Table 1.

[SIDE BAR: The different analytical methods for measuring NO have resulted in inconsistent reporting of limit of detection (LOD) ranging from concentration (e.g., μM or nM) to absolute amount (e.g., pmol, ppm). Such inconsistency is partially due to NO being measured as a gas (in ppb or ppm) and as a dissolved species (in molar units). Every effort has been made to maintain consistency to allow comparison between techniques.]

2. SPECTROSCOPIC METHODS

2.1. Absorbance-based measurements

Absorbance-based methods for the detection of NO benefit from simple and affordable instrumentation, and conceptually straightforward analysis procedures. As such, they are widely used for detecting NO, especially in biological systems.

2.1.1. Metalloprotein-based assays—First reported by Haussmann and Werringloer (21) as a method for the quantitative detection of NO, the hemoglobin assay involves the reaction of oxyhemoglobin (HbO_2) and NO to produce methemoglobin (MetHb) and nitrate with a concomitant spectral shift:

$$\text{Hemoglobin-Fe(II)-}O_2 + NO \rightarrow \text{Hemoglobin-Fe(III)} + NO_3^-$$

The progress of the reaction may be monitored spectrophotometrically by measuring the absorbance at 401 nm (MetHb) and 415 – 421 nm (HbO_2). Details of this analytical technique have been reviewed by Noack et al. (22) and Murphy et al. (23). The reaction is nearly diffusion-limited (23,24) and 26 times faster than the reaction between NO and O_2 (22), allowing for the measurement of NO in the presence of dissolved O_2. Interference from other nitrogen oxides is not observed. Each experiment requires a separate calibration that may be conducted either via oxidation of HbO_2 with potassium ferricyanide, with an NO donor that generates a known quantity of NO, or by addition of a saturated NO solution. Quantitative results are obtained by monitoring the difference in absorbance between 401 and 411 nm. Control solutions of HbO_2 alone must be run simultaneously to account for HbO_2 autoxidation. The theoretical detection limit is 1.3 – 2.8 nM (22,23). Interferences may arise from fluctuations in temperature, the presence of other heme-containing proteins, and changes in pH, each of which may influence the absorbance spectrum of MetHb. The

presence of other redox-active species may also interfere with the measurement, as oxidation of HbO_2 and/or reduction of MetHb will affect the assay (22). A primary drawback of this technique is the need for fresh HbO_2 reagent (23), obtained via time-consuming oxygenation of hemoglobin followed by chromatographic purification (25).

The hemoglobin absorbance-based technique has been used to detect NO released from exogenous NO donors (23), cultured endothelial cells (26), platelets (27) and tissue (28,29). For example, Zhang et al. coupled the hemoglobin assay with intracerebral microdialysis to measure NO levels in rat brains (29). Cellulose membrane coaxial microdialysis probes (5000 MW cut-off) were inserted into the hippocampus of anesthetized rats and perfused with Krebs buffer containing 10 μM HbO_2. Spectral shifts in the collected microdialysate indicated increased NO production in the brain after administration of kainic acid, an excitotoxin responsible for increased NO production (29). Autoxidation of hemoglobin was minimized by maintaining the perfusate at 0 °C prior to entry into the microdialysis probe. The limit of detection for the assay was 7 nM (29). With minor modifications, microdialysis coupled with the hemoglobin assay may be useful for monitoring NO levels in other tissues and organs as well.

In a recent advance, Boon & Marletta reported a new metalloprotein assay for detecting NO using a mutant of *Tt* H-NOX, a bacterial heme protein with significant homology to guanylate cyclase (30). The researchers introduced a point mutation (Y140F) that significantly decreased the affinity of the protein for O_2 while maintaining high affinity for NO, thus better enabling its use under aerobic conditions. The protein, *Tt* Y140F, was found to be a cumulative trap of NO, allowing the measurement of NO by monitoring the change in absorbance at 424 nm. Based on the change in extinction coefficient of the protein at 424 nm with and without bound NO, the concentration range over which NO could be detected was 300 nM to 30 μM. The authors employed the *Tt* Y140F assay to determine the amount of NO released from murine inducible nitric oxide synthase. Of note, the *Tt* Y140F was stable up to 70 °C and tolerated salt and buffer (30).

Heme-containing proteins other than hemoglobin are also suitable for quantitative NO detection based on absorbance changes after reaction with NO. For example, Aylott et al. created an optical NO sensor by trapping cytochrome *c* in a 5-μm thick tetramethylorthosilicate (TMOS) xerogel spin-coated on a glass substrate (31). The protein-doped xerogel film was affixed to a gas flow cell normal to the light path of a spectrophotometer. Absorbance measurements indicated that NO binding caused a shift in λ_{max} from 406 to 414 nm. The sensor generated a linear response to NO from 1 – 25 ppm, with a limit of detection of 1 ppm and a relative standard deviation of less than 1% at 10 ppm. While no interference was observed from O_2, nitrogen gas (N_2), or carbon monoxide (CO), introduction of nitrogen dioxide (NO_2) at 10 – 1000 ppm did result in an interfering signal (31).

In a similar manner, Lan et al. developed optical sensors for NO based on manganese myglobin (MnMb) encapsulated in a TMOS xerogel matrix (32). Specificity for NO over O_2 was achieved by employing MnMb, which unlike native myglobin binds NO but not O_2 (33). The MnMb-doped TMOS xerogels were placed in aerobic solutions containing NO generated either enzymatically from nitric oxide synthase or from *S*-nitroso-*N*-acetylpenicillamine (SNAP), a small molecule NO donor. Absorption spectra recorded before and after exposure to NO indicated a change in λ_{max} from 468 nm (Mn(III)Mb) to 424 nm (Mn(II)MbNO). Although the sensitivity and limit of detection of the sensor were not reported, the technique was found to be specific for NO over both nitrite (NO_2^-) and nitrate (NO_3^-), but not nitroxyl (HNO) or NO_2 (32).

2.1.2. Other absorbance assays with metal-based indicators—Metal-based indicators other than metalloproteins have also received attention due to their potential for NO detection. For example, Dacres & Narayanaswamy developed optical NO sensors based on absorbance changes of Cu(II) complexes upon exposure to NO (25,34,35). Initial studies focused on a copper-eriochrome cyanine R complex [Cu(II)-ECR] that in the absence of NO exhibited a λ_{max} of 445 nm in buffer. Upon exposure to NO, the absorbance at 445 nm decreased with a concomitant increase in absorbance at 569 nm due to reduction of the complex from Cu(II)-ECR to Cu(I)-ECR (25). To make use of this finding for developing an optical sensor for NO, the Cu(II)-ECR complex was immobilized in a silicone rubber membrane and cast as a film into a gas flow cell equipped with a fiber optic-based spectrometer. The immobilized complex exhibited spectral characteristics different than that in solution, with NO exposure resulting in a λ_{max} shift from 580 to 610 nm, and a decrease in absorbance. Nevertheless, the optical sensor proved suitable for monitoring NO gas with a limit of detection of 0.23 ppm NO and linear response up to 6 ppm (25). The authors have since developed an improved sensor by immobilizing the Cu(II)-ECR complex in an anion exchange membrane (35). While the limit of detection for the new immobilization strategy improved to 0.848 ppm NO, the sensitivity increased almost 5-fold compared to the silicone rubber-based sensor. The response of the anion exchange sensor was also reversible and selective for NO over O_2, NO_2, and CO (35).

2.1.3. Diazotization assay (Griess reaction)—One of the most common methods for detecting NO from a wide variety of samples and matrices is the diazotization or Griess assay. First described by Griess in 1864 (36), the diazotization assay actually measures nitrite. Fortunately, NO's reactivity results in the formation of nitrite in oxygenated media via the following reactions:

$$2NO + O_2 \rightarrow 2NO_2$$

$$NO + NO_2 \rightarrow N_2O_3$$

$$N_2O_3 + H_2O \rightarrow 2NO_2^- + 2H^+$$

Review articles describing the procedures for detecting NO via the Griess reaction and its application to biological samples are available (37,38). Nevertheless, we provide a brief description of the fundamentals of this NO measurement technique.

The original reaction developed by Griess involved reacting nitrite with sulfanilic acid and α-naphthylamine under acidic conditions to yield an azo dye whose concentration could be used as an indirect indicator of nitrite (and NO) concentration in the sample (38). The assay was later modified (39) to the procedure used widely today by substituting sulfaniliamide (SA) and *N*-(1-naphthyl)ethylenediamine (NED) for sulfanilic acid and α-naphthylamine, respectively. This modification resulted in greater sensitivity and reproducibility, and more rapid analysis times (38). As shown in Figure 1, the modern version of the Griess reaction involves first reacting nitrite with SA under acidic conditions to form a diazonium salt intermediate (37,38). The diazonium salt intermediate is then coupled to NED to form the stable water-soluble azo dye ($\lambda_{max} \approx 540$ nm). Nitrite concentration is determined by comparing the absorbance of the azo dye solution to a calibration curve prepared with known concentrations of nitrite. The limit of detection for nitrite via the Griess assay is approximately ~0.5 μM (37). Since the Griess assay detects a byproduct of NO (i.e., nitrite), it is not suitable for monitoring NO in real time. Furthermore, careful control experiments must be performed to distinguish basal nitrite levels from those due to changes in NO concentrations.

Variations in the assay exist due to the multi-step nature of the reaction. In some cases, the sample is incubated with hydrochloric acid (HCl) and SA for 10 min followed by addition of

NED and further incubation (30 min) before measuring the absorbance (40). It is also possible to add the sample directly to an acidic solution containing both SA and NED. However, most commercially-available kits call for the sample to be mixed with SA followed by immediate addition of NED, which has been reported to be the most sensitive method of nitrite determination (37).

In addition to NO_2^-, the reactions of NO in oxygenated solutions may also yield nitrate (NO_3^-) via the following reactions:

$$2NO + O_2 \rightarrow 2NO_2$$

$$2NO_2 \rightarrow N_2O_4$$

$$N_2O_4 + H_2O \rightarrow NO_2^- + NO_3^- + 2H^+$$

As a competing reaction that lowers the amount of NO_2^- produced from NO, NO_3^- formation represents a significant interference for quantitative determination of NO via the Griess assay. Fortunately, the reactions that culminate in NO_3^- production are slower than those leading to NO_2^- (40), and thus NO_2^- is considered to be the major NO byproduct in oxygenated solutions. Nevertheless, since the Griess assay does not detect NO_3^-, it may be necessary to first reduce any NO_3^- present to NO_2^- for complete analysis. Methods for NO_3^- reduction (to NO_2^-) include treatment with chemical reductants such as cadmium, zinc, and vanadium chloride. Enzymatic reduction may also be employed via NO_3^- reductase obtained from bacteria (41). However, the enzymatic approach requires NADPH as a cofactor, which has been shown to interfere with the Griess assay (42).

As a common method for measuring NO in biological systems, applications of the Griess assay are too numerous to permit a comprehensive overview. Rather, we point the interested reader to a recent review describing applications of the Griess assay for elucidating the mechanisms of NO's action in physiology (38) and to select research articles in which the Griess assay has been used to measure nitrite as a proxy for NO in urine (43), cerebrospinal fluid (44), plasma (45), serum (46), and blood (47). The Griess assay has also been used to quantify solution NO release from NO donors such as linsidomine (SIN-1) (48), sodium nitroprusside (49), poly(ethylene glycol)-lysine dendrimers (50), and self-assembling diazeniumdiolate-based nanofiber gels (51).

Analytical applications of the Griess assay continue to expand with the development of new instrumentation for measuring NO based on the Griess reaction. Several reports have appeared describing absorbance-based flow injection analysis systems for the measurement of NO via the Griess reaction (52–54). For example, Higuchi et al. (54) describe a system where the carrier solution (with sample) is first passed through an on-line copperized cadmium reduction column to reduce NO_3^- to NO_2^-. The NO_2^- then reacts with SA and NED in a heated (50 °C) reaction column. Using this system, the authors determined NO_2^- levels in urine, serum, plasma, and cell culture samples. A 50 nM limit of detection was reported with linear calibration responses up to 10 μM NO_2^-.

Likewise, Toda et al. (55) developed new instrumentation for monitoring gaseous NO via the Griess reaction. A micro-gas analysis system was developed that operates by passing a gas-absorbing solution (3% aqueous triethanolamine) through a microchannel scrubber formed on polydimethylsiloxane coated with a porous polytetrafluoroethylene membrane. After collecting sample from the scrubber, the gas-absorbing solution is reacted with Griess reagent and passed through a reaction coil maintained at 50 °C. The solution is then introduced to a 1-cm path length detector with a 525-nm LED and a high sensitivity photodiode. The limit of detection of the NO microanalysis system was 7 ppb with a linear response to 1 ppm, although NO concentrations as high as 50 ppm may be determined with a

multipoint calibration. The Griess assay-based instrument should prove useful for both environmental monitoring and medical applications (55).

2.2. Fluorescence-based measurements

A number of fluorescence-based probes have been developed for the detection of NO and a recent review highlights the mechanisms by which they operate and their applicability for biological applications (56). Fluorescence probes are particularly useful for monitoring the spatial and temporal aspects of NO production. Most probes exhibit little or no fluorescence until reacted with a byproduct of NO decomposition (e.g., N_2O_3) after which they become highly fluorescent, with the exception of fluorescent nitric oxide cheletropic traps (FNOCTs). FNOCTs are *o*-quinodimethane derivatives that react directly with NO to produce a nitroxide radical product with significantly different fluorescence properties (e.g., intensity and/or wavelength) than the original FNOCT. Since their fluorescence is not dependent on a byproduct of NO decomposition, they are suitable for unambiguously indicating the presence of NO (56,57). Meineke et al. employed FNOCTs to both measure NO release from cultured macrophages and image intracellular NO production by endothelial cells via fluorescence microscopy (58). Similar fluorescent probes that react directly with NO include metal-based compounds synthesized by Lippard and coworkers (59). Such probes include Co(II), Fe(II), Ru(II), Rh(II) and Cu(II) compounds that are directly sensitive to NO and not an oxidation byproduct (59). The detection limit of the Cu(II) fluorescein complexes is roughly 5 nM (60) and is suitable for visualizing NO production from both human neuroblastoma cells and murine macrophages (61).

Diaminofluoresceins (DAFs), first described by Kojima et al. in 1998 (62,63), are among the most widely-employed NO-sensitive fluorescent probes because of their utility for cellular imaging. Upon reaction with a byproduct of NO (i.e., N_2O_3), the fluorescence intensity of the DAF probes increases by approximately 100-fold (63). In addition to having visible excitation wavelengths similar to fluorescein (an advantage for cellular applications), a diacetate-derivatized form (DAF-2 DA) allows for efficient uptake by cells. Hydrolysis of the acetate bonds by intracellular esterases results in a trapped non-permeable form of the probe (DAF-2) (56,63). The DAF probes show no fluorescence in the presence of common interferents for NO such as NO_2^-, NO_3^-, hydrogen peroxide (H_2O_2), and peroxynitrite ($ONOO^-$), and have a detection limit as low as 5 nM (63). Examples of using DAF probes include quantifying changes in NO production in stimulated perfused rabbit hearts (64) and imaging NO production in living zebrafish (65).

Diaminofluorescein probes have also been coupled with analytical techniques such as flow cytometry for analysis of NO production by cells. For example, Stirjdom et al. used DAF-2 DA and flow cytometry to monitor intracellular NO in cardiomyocytes treated with either diazeniumdiolate-modified diethylamine (DEA/NO), a NO donor, or subjected to simulated ischemia (hypoxia) (66). In a similar study, DAF-2 DA was coupled with flow cytometry to measure NO in human lung and liver epithelial cells (67). The authors compared the amount of NO assayed from the DAF/flow cytometry experiment to NO measured by both the citrulline assay (i.e., measuring L-arginine conversion (68)) and by reducing nitrite and nitrate to NO followed by chemiluminescent NO detection (see Section 2.3). Good correlation was observed between the assays, thereby validating the DAF/flow cytometry approach with established methods of cellular NO detection. Of note, incubation of cells with higher concentrations of DAF-2 DA (250 μM) increased the sensitivity of the assay. However, DAF-2 DA concentrations above 10 μM have been found to be toxic to some cells (67).

Fluorescent dyes have also been coupled with both high-performance liquid chromatography (HPLC) and capillary electrophoresis for the sensitive detection of NO. For example, Huang

et al. (69) developed a technique whereby NO was reacted with 1,3,5,7-tetramethyl-8-(3′, 4′-diaminophenyl) difluoroboradiaza-*s*-indacene (TMDABODIPY) prior to injection onto a non-polar octadecylsilane (C_{18}) HPLC column. Using fluorescence detection ($\lambda_{ex}/\lambda_{em}$ = 498/507 nm), baseline separation between reacted and unreacted TMDABODIPY was observed within 4 min, with a linear response to NO and limit of detection of 0.8 – 800 nM and 20 pM, respectively. The method was applied to measure NO in serum of patients with ischemic cardio-cerebrovascular disease (69). As an improvement over the original procedure, a solid-phase microextraction method was employed to pre-concentrate the TMDABODIPY-derivatized NO prior to HPLC analysis (70). Use of a poly(methacrylic acid-ethylene glycol dimethacrylate) (MAA-EGDMA) monolithic extraction column improved the limit of detection to 2 pM and allowed for the measurement of NO in rat heart, kidney, and liver samples (70).

Capillary electrophoresis (CE) has been employed to improve the selectivity of DAF probes for NO over common intracellular inteferents (71). Intracellular ascorbic acid is known to reduce levels of N_2O_3, the NO reaction byproduct responsible for generating the fluorescent form of DAF (63). Moreover, dehydroascorbic acid reacts with DAF to yield a product with similar fluorescence properties as the desired DAF reaction product with N_2O_3 (72). To minimize the interfering effects of both intracellular interferents, Kim et al. employed ascorbate oxidase (AO) to catalyze the oxidation of ascorbic acid to dehydroascorbic acid and water, thus removing the N_2O_3 scavenger (i.e., ascorbic acid). Capillary electrophoresis was then employed to separate the DAF–N_2O_3 reaction product from the fluorescent DAF–dehydroascorbic acid product. The CE method allowed for the successful measurement of NO from *Aplysia californica* metacerebral cells, effectively separating the DAF–N_2O_3 reaction product from unidentified neuron-specific interferents (71).

The inherent fluorescence of select proteins is also sensitive to NO. To exploit this property, Barker et al. made use of the fluorescence attenuation of cytochrome *c*′ upon NO binding to create NO sensitive optical sensors. Upon NO binding, the fluorescence intensity of *Chromatium vinosum* cytochrome *c*′ decreased and exhibited a ~10 nm blue shift ($\lambda_{excitation}$ = 530 nm) (73). Sensors were fabricated by photopolymerizing a 9:1 (w/w) (acrylamide) : (*N,N*-methylenebisacrylamide) solution with *C. vinosum* cytochrome *c*′ onto multimode optical fibers. Using 10 mW 514.5-nm Ar^+ laser excitation, a linear response to NO was observed up to 1 mM. Due to an irreversible response thought to arise from NO's reaction with the polymer matrix (73), the authors coated the sensor with a layer of gold colloid onto which cytochrome *c*′ was adsorbed via protein amine groups. The sensors exhibited full reversibility with a limit of detection of 20 μM and linear response to 1 mM, with a second linear response region above 1 mM. A response time of ~0.9 s was reported with minimal interference from NO_2^-, NO_3^-, O_2, N_2, or ascorbic acid (73).

In addition to protein-based sensors, optical NO sensors have also been developed based on synthetic NO-sensitive fluorescent probes. For example, Kopleman's group fabricated fluorescence-based NO sensors by immobilizing 4-carboxy-2′,7′-difluorofluorescein (Oregon Green 488) dye onto the 50-nm gold colloid prior to coating optical fibers (74). Although Oregon Green 488 in solution is insensitive to NO, when immobilized on gold its fluorescence intensity is attenuated upon NO co-adsorption to the gold surface. Carboxylate-modified polystyrene fluorescent microspheres (40 nm) insensitive to NO were also incorporated as part of the sensor, allowing the ratiometric measurement of NO by normalizing the change in Oregon Green 488 fluorescence intensity to that of reference microspheres. The analytical response of such sensors was characterized by a 20 μM NO limit of detection, linear response up to 1 mM NO, and <0.25 s response time (0–100% response). Although no interference was observed from NO_2^- (1 M), NO_3^- (1 M), 100% O_2, or $[H^+]$ at pH > 6, slight (≤ 4% signal change) interference was noted from hydrogen

peroxide (18 μM), superoxide (3 μM), and peroxynitrite (6 μM). The Oregon Green 488/colloidal gold sensors were used to monitor NO release from resting and stimulated murine macrophages by placing the sensor ~0.5 cm from cultured cells. A ~5-fold increase in NO production (from < 20 to 190 ± 70 μM) was measured upon stimulation of the macrophages with interferon-γ and lipopolysaccharide (74). Similar fluorescence-based NO sensors were also fabricated by labeling cytochrome *c*′ with Oregon Green 488 prior to attaching the protein/label conjugate to gold colloid-coated fibers that were co-immobilized with reference polystyrene microspheres (75). The dual protein/dye sensor exhibited similar analytical response as the previously-developed protein- and dye-only sensors, with the exception of an improved limit of detection (8 μM NO) (75).

2.3. Chemiluminescence

Two types of chemiluminescent reactions have been employed to selectively detect NO. As shown below, the first approach is based on the reaction of NO with ozone (O_3) in a reaction cell to produce excited state nitrogen dioxide (NO_2*), which emits a photon upon relaxation to the ground state:

$$NO + O_3 \rightarrow NO_2^* + O_2$$

$$NO_2^* \rightarrow NO_2 + h\nu$$

Described in a review by Bates (76), the ozone-based chemiluminescent reaction is highly specific for NO, although NO_2^- and NO_3^- may be measured upon their reduction to NO. The emitted light is measured with a photomultiplier tube (PMT) with the intensity proportional to the amount of NO in the reaction cell. While interferences may arise due to chemiluminescence from the reaction of O_3 with species such as ethylene hydrocarbons, sulfur compounds, and carbonyls, the wavelength of chemiluminescence provides an effective method for discriminating between such interferents. Indeed, ethylene reaction with O_3 results in chemiluminescence at ~440–470 nm while sulfur compounds result in chemiluminescence at <400 nm. In contrast, the NO/O_3 reaction emits light at wavelengths >600 nm, allowing the use of a simple filter to remove undesirable signal and impart complete selectivity for NO (76). As shown in Figure 2, the most commonly-employed ozone-based chemiluminesce NO detectors use an inert gas (e.g., Ar or N_2) to both deoxygenate the sample solution and carry gaseous NO from a sample vessel through a cold trap (to remove water vapor) and into a reaction cell. In the reaction cell, the NO reacts with O_3 generated from O_2 either directly from air or from a dedicated oxygen tank. After passing through a filter, light from the chemiluminescent reaction is then measured via a PMT. The major advantage of employing a carrier gas is that the most troublesome interferents (e.g., NO_2^- and NO_3^-) are not transferred from the sample vessel to the reaction cell, enhancing NO selectivity. However, this measurement mode is susceptible to changes in the flow rate of the carrier gas and only suited for detecting gaseous NO, making it incompatible with many biological experiments (76). The limit of detection for solution-based samples is in the nM–pM range (depending on the sample volume) (76), with an analysis range to mM levels (77). For gas samples, the detection limit is 0.5 ppb and with an analysis range to ~500 ppm (77). The analysis range for solution excellent sensitivity, and near-real time monitoring of NO have resulted in chemiluminescence being widely employed for NO detection. Indeed, several reports have detailed the use of ozone-based chemiluminescence for measuring NO from NO-releasing materials such as silica nanoparticles (78), nitrosothiol-modified dendrimers (79), and xerogel polymers (80), as well as from biological samples such as human arterioles (81), and in exhaled breath (82).

The second method of chemiluminescent NO detection, initially described by Kikuchi et al. (83), is based on the reaction of NO with hydrogen peroxide (H_2O_2) to form peroxynitrite ($ONOO^-$), which subsequently reacts with luminol to yield characteristic

chemiluminescence. In the initial assay, samples containing NO were added to luminol solution (30 μM) pre-mixed with H_2O_2 (10 mM). A linear calibration curve was obtained for NO concentrations from 100 fM to 1 nM. Possible interferents such as NO_2^- and NO_3^- were found to give no chemiluminescent signal, while the addition of NO_2 resulted in a small signal (<5% of the signal obtained from NO) (83). Coupled with a flow cell-type detector, luminol chemiluminescence has been used to measure NO from a perfused rat kidney and correlate NO levels with arterial perfusion pressure (83).

The luminol/H_2O_2 chemiluminescence approach has also been employed to create analytical sensors for NO. For example, Robinson et al. developed a chemiluminescence-based technique for measuring NO in exhaled breath (84). Porous polypropylene hollow fiber membranes were used to channel gaseous NO into a solution of luminol and H_2O_2 from which chemiluminescence was detected with a miniature photomultiplier tube. The instrument was characterized as having a limit of detection of 0.3 ppb. At this level, the authors suggested that it may find application for monitoring NO as a diagnostic marker for asthma or respiratory infections (84). In similar work, Zhou et al. developed a luminol-based chemiluminescence fiber optic sensor for measuring NO in solution (85). A solution containing luminol and hydrogen peroxide was trapped at the end of a fiber optic probe with a gas permeable membrane (nonvulcanized matte-matte silicone sheeting). Light emission from the chemiluminescent reaction was transferred through the fiber to a PMT for detection. The optical sensor was characterized as having a limit of detection of 1.3 μM NO, linear response to 40 μM, and a response time of 10–17 s. Physiological substances that reduced ambient oxygen were found to increase the response of the sensor by inhibiting the oxidation of NO. Both thiols and carbon monoxide (CO) were also found to significantly interfere with the sensor response to NO (85).

2.4. Electron paramagnetic resonance spectroscopy

Electron paramagnetic resonance (EPR) or electron spin resonance (ESR) spectroscopy has proven particularly useful for detecting NO in complex biological matrices such as tissues and organs. Radical species with unpaired electrons such as NO are readily observed in magnetic fields based on the absorption of electromagnetic radiation in the microwave region that induces resonance between parallel and anti-parallel orientations relative to the applied magnetic field (86). The EPR signal is typically reported as the first derivative of the absorption spectrum. Modern EPR instruments hold the microwave frequency fixed and scan the magnetic field strength until resonance between the parallel and anti-parallel states is reached and a signal is observed. As with nuclear magnetic resonance (NMR) spectroscopy, atoms with a magnetic moment that neighbor the atom with the unpaired electron will influence the EPR signal via hyperfine coupling. Both qualitative and quantitative information may be obtained from EPR.

As a free radical with an unpaired electron, NO is readily monitored via EPR spectroscopy. Since EPR is only sensitive to free radical species, EPR as a NO measurement method is highly selective over common interferents such as NO_2^- and NO_3^-. However, since NO is characterized by a short half-life in biological milieu and rapidly reacts to form non-paramagnetic species, it is necessary to “trap” NO and convert it to a more stable radical species for monitoring. As shown in the following reaction, spin trapping involves reacting a free radical with a “spin trap” reagent to form a stable adduct that may be monitored via EPR:

$$R^* + ST \rightarrow R\text{-}SA^*$$

where R* is the radical to be monitored, ST is the spin trap, and R-SA* is the stable radical trap adduct (86). A review by Kleschyov et al. describes the measurement of NO via spin trapping and EPR (86). Both endogenous and exogenous spin traps exist for NO detection,

and both have been employed for monitoring NO's role in biological applications (86). Below, representative examples of EPR and spin traps for monitoring NO, and the information obtainable from such analyses are provided.

2.4.1. Endogenous spin traps—Of the endogenous NO spin traps, hemoglobin has proven particularly useful. While the major reaction product of oxyhemoglobin and NO is methemoglobin and NO_3^- (the basis of the hemoglobin assay for NO described above), approximately 10% is converted to a stable HbNO adduct. Dikalov & Fink reported the use of HbNO to monitor NO via EPR in both whole blood and erythrocytes. Calibration was performed by incubating washed erythrocytes with known amounts of either NO_2^- or diazeniumdiolate NO donor. This EPR technique was then employed to monitor HbNO levels in mice fed low and high nitrite/nitrate diets (87). In a similar study, Hall et al. used ex vivo EPR analysis of HbNO and methemoglobin (also paramagnetic) combined with Griess analysis to conclude that hyperthermia in rats resulted in increased production of NO at levels similar to those observed during septic shock and endotoxin administration (88).

Similar to hemoglobin, alternative endogenous spin traps for NO include other metalloproteins in tissue such as myoglobin, cytochrome C, catalase, and cyclooxygenase (86). While NO-heme complexes are paramagnetic and detectable by EPR, O_2- and CO-heme complexes are diamagnetic and thus not observable by EPR, representing yet another layer of EPR selectivity for NO (89). Using heme proteins as endogenous spin traps, Kuppusamy et al. employed EPR to both measure and image NO generation in mice subjected to cardiopulmonary arrest (90). As expected, increased NO production was observed in the mice suffering cardiopulmonary arrest. The mechanism of NO production was determined by administering ^{15}N-labeled nitrite (i.e., $^{15}NO_2^-$) to the mice (as NO derived from $^{15}NO_2^-$ may be distinguished from enzymatically-generated NO via EPR analysis). The majority of NO was produced non-enzymatically from the acidic reduction of tissue nitrite. Double integration of the EPR signal from individual organs allowed the location of NO production to be determined, with the greatest NO produced in the lungs and heart. Whole-body imaging obtained by collecting serial EPR spectra confirmed the spatial distribution of NO production in the lungs, heart, and liver (90).

2.4.2. Exogenous spin traps—The most common exogenous NO spin-traps are iron-dithiocarbamates, which have proven particularly useful for monitoring NO in cells and tissue (86,91) including animal tumors (92), kidneys (93), mouse organs (94,95), and plants (96). As with endogenous heme protein spin traps, iron-dithiocarbamates also allow imaging of NO production in live animals (97). The use of iron-dithiocarbamates to facilitate EPR detection of NO has been the subject of several reviews (98,99), and exploits the high affinity of NO for the Fe center of the spin trap. The general structure of iron-dithiocarbamates is $Fe(S_2CN\text{-}RR')_2$, where R and R′ can be methyl-, ethyl-, glucamine-, sarcosine- (86,97,100–102), or amino acid substituents such as proline or serine (103–105). The identity of the substituents dictates the regions in animals or tissues where NO may be most readily detected. For example, the lipophilic Fe-diethyldithiocarbamate (DETC) accumulates in hydrophobic membranes, making it suitable for detecting NO in tissue. In contrast, the more hydrophilic Fe-*N*-methyl-D-glucamine dithiocarbamate (MGD) remains in the extracellular fluid and is thus more useful for measuring NO outside of cells (86). The detection limit of NO using exogenous spin traps is roughly 6 pmol (rat thoracic aorta sample) (106).

3. ELECTROCHEMICAL TECHNIQUES

The electrochemical sensor is likely the most commonly employed analytical method for monitoring NO in physiology/biology due to specific inherent advantages including real-

time monitoring, amenability to miniaturization, and the ability to enhance selectivity and sensitivity via electrode modification and/or the applied potential (107). Moreover, electrochemical detection of NO affords excellent spatial resolution with extraordinarily low limits of detection. Indeed, porphyrinic-based NO microsensors have been used to detect as little as 10^{-20} moles of NO in single cells (108,109). While electrochemical reduction of NO may be employed for NO detection (107,110–113), it is often plagued by the threat of interference from oxygen, whose reduction occurs more readily than that of NO (107,114). As a result, the majority of electrochemical NO sensors are based on the oxidation of NO to nitrite. Unfortunately, the relatively high working potential required to oxidize NO (+0.7 to 0.9 V vs. Ag/AgCl, depending on the type of electrode (115)) may lead to interference from other redox-active species such as NO_2^-, ascorbic acid, uric acid, dopamine, and carbon monoxide (CO) common to physiological milieu. As such, bare electrodes are often modified to reduce interferences and facilitate selective detection of NO. The two primary electrode modification include: 1) coating the electrode with a membrane that selectively allows the diffusion of gases while excluding other interferents; and, 2) modifying the electrode by immobilization of an electrocatalytic compound such that the potential necessary to oxidize NO is lowered compared to that of the interferents.

The Shibuki NO sensor is among the first examples of a membrane-coated electrochemical NO sensor (116). As shown in Figure 3 A, a Teflon-coated platinum (Pt) working electrode and Pt reference electrode were placed in a glass micropipette filled with NaCl/HCl solution prior to sealing one open end of the pipette with NO-permeable chloroprene rubber. Nitric oxide was detected via oxidation at +0.8 to +0.9 V versus a Ag/AgCl reference electrode. The response of the sensor was linear from 1 to 3 μM NO with a sensitivity of 28.3 ± 4.4 pA/μM. Shibuki first used the sensor to monitor NO generation from sodium nitroprusside (a chemical NO donor), and then from electrically-stimulated rat cerebellar slices. Several permselective membranes have since been employed to fabricate electrochemical sensors with analytically useful selectivity. Examples of such membranes include cellulose acetate (117), collodion/polystyrene (118), polycarbazole (119), Nafion (120), polyeugenol (121), polydimethylsiloxane (122), poly(tetrafluoroethylene) (123), and phenylenediamine (124).

The first use of an electrocatalytic modification for reducing the potential necessary to oxidize NO was reported by Malinski & Taha in 1992 (108). A p-type semi-conducting nickel porphyrin film was applied to a thermally sharpened carbon fiber microelectrode prior to coating the electrode with Nafion. The oxidation potential of the sensor for NO was lowered to approximately +0.65 V, a clear indication of the catalytic properties of the Ni porphyrin (107,108). The sensor had a limit of detection of 10 nM NO and responded linearly to NO up to 300 μM, allowing for the determination of NO release from single porcine aorta endothelial cells (108). Other approaches for electrocatalytically lowering the oxidation potential of NO include modifying electrodes with metalloporphyrins (125), metal phthalocyanines (126,127), and other organometallic compounds with Ni, Fe, Co, Cu, and Mn centers (128–130). A review highlighting sensors fabricated using both permselective membranes and electrocatalytic modifications was published in 2003 (131). The advances discussed herein represent more recent work and new strategies designed to improve selectivity over interferents.

3.1. Platinization and permselective membranes for enhancing the response of electrochemical NO sensors

Much literature details the use of polymeric sensor membranes for improving the selectivity for NO over common interferents. For example, Lee et al. designed an amperometric NO sensor using a platinized Pt electrode coated with a microporous poly(tetrafluoroethylene) (PTFE) gas-permeable membrane (132). The process of platinization has been employed since the 1800s (133) to improve electrochemical sensor response characteristics such as

sensitivity and limit of detection by increasing surface area and enabling faster electron transfer kinetics between the electrode and analyte (132). Platinum working electrodes were platinized in a 3% chloroplatinic acid solution and placed with a coiled Ag wire reference electrode in a glass micropipette. A PTFE gas-permeable membrane was affixed to the distal end of the sensor with an O-ring. The effect of platinization on the oxidation potential of NO was determined via linear sweep voltammetry. Electrode platinization was found to increase the sensor response (i.e., current) for both NO and NO_2^- by ~8-fold compared to unplatinized electrodes. Furthermore, the platinized electrodes enabled faster electron-transfer kinetics for both NO and NO_2^-, allowing the oxidation potential to be reduced to +0.75 V while maintaining the same sensitivity to NO as sensors operated at +0.9 V. Platinization also improved the lifetime of the sensor, as platinized sensors exhibited no change in response (within ±10%) after 3 d, while the sensitivity of non-platinized sensors was reduced by ~50% after only 3 h. The response time of the sensor (i.e., time required to reach 90% of steady-state response when [NO] was changed from 10 to 400 nM) was 14–25 s, while the limit of detection was 1 nM NO. Furthermore, the PTFE membrane resulted in complete selectivity over nitrite up to 10 mM NO_2^- concentrations (132). Unfortunately, ammonia (NH_3) was found to interfere with sensor response (134). To overcome this interference, the PTFE-based sensor was modified by applying a Teflon AF® (i.e., 2,2-bis(trifluoroethylene)-4,5-difluoro-1,3-dioxole) coating over the PTFE membrane. The Teflon AF® layer improved the sensor selectivity for NO over ammonia by ~1000-fold (134).

To reduce the size of NO sensors, the Schoenfisch research group developed xerogel-based perselective membranes (115,135). Sol-gel-derived materials (i.e., xerogels) are formed via the hydrolysis and condensation of alkoxysilanes under relatively mild synthetic conditions. Such materials are characterized by unique chemical versatility based on precursor selection and the ability to adhere to many substrates (115). In the first report of xerogel-based electrochemical NO sensors, Shin et al. employed amino- and alkyl-alkoxysilanes as xerogel precursors and a NO templating strategy following the formation of the xerogel. The optimum membrane composition, based on permeability to NO and selectivity to NO over nitrite, consisted of (aminoethylaminomethyl)-phenethyltrimethoxysilane (AEMP3, 20% v/v, balance methyltrimethoxysilane [MTMOS]) doped with 17% (v/v to total silane) Nafion. The Nafion both enhanced NO permeability and selectivity for NO over NO_2^- and other interferents. The selectivity coefficients (log $K_{NO,\,j}$) of the resulting NO sensor were −5.8, < −6, <−6, and <−6 for j=nitrite, ascorbic acid, uric acid, and acetaminophen, respectively. Other notable sensor performance characteristics included a response time (i.e., $t_{95\%}$ 400 to 500 nM NO) of 9 s, a limit of detection of 25 nM, a sensitivity of 0.17 pA/nM, and a linear response to 15 μM (115). Notwithstanding, the membrane conditioning steps prior to NO measurement were cumbersome.

To simplify the sensor fabrication protocol, Shin et al. (135) replaced the amino-alkoxysilane precursor with fluoroalkoxysilane, a “PTFE-like” polymer precursor. In contrast to the previously-developed PTFE-based sensors (132,134), the fluorinated xerogels provided a more straightforward and reproducible method for coating the working electrode. Indeed, a benefit of sol-gel chemistry is the ability to dipcoat thin layers of the xerogel onto electrodes. The optimal membrane composition consisted of a ~10 μm-thick (heptadecafluoro-1,1,2,2-tetrahydrodecyl)trimethoxysilane (17FTMS, 20% v/v)/methyltrimethoxysilane (MTMOS) xerogel film, resulting in a more hydrophobic membrane with a water contact angle of ~104°. The NO selectivity (log $K_{NO,\,j}$) of sensors constructed with such membranes over common interferents was −1.33, −5.74, and −5.84 for j = carbon monoxide, nitrite, and ammonia/ammonium, respectively, and <−6 for j = ascorbic acid, uric acid, acetaminophen, and dopamine (135). The NO permeability ($\Delta I_{xerogel}/\Delta_{bare}$) of the fluorinated xerogel membrane was significantly enhanced compared to the aminosilane-

based xerogel membranes (0.72 versus 0.1, respectively, for 10 μM NO) (115). As shown in Figure 3 B, NO microsensors were subsequently fabricated by coating platinized Pt/W microelectrodes with the optimized fluorinated xerogel membrane. The analytical performance of such sensors included a limit of detection of 83 pM NO, a response time of <3 s, a sensitivity of 7.91 pA/nM, and a linear response to 4 μM. Furthermore, the sensors maintained >90% of the initial sensitivity after storage for 20 d in phosphate buffered saline at room temperature. In total, the performance of the fluorosilane-based NO sensors surpassed that of many previously-developed miniaturized NO sensors (135). Of note, the Ag/AgCl reference electrode was separate from the working electrode in contrast to the larger Shibuki-based devices.

3.2. Electrocatalytic sensor modifications

In addition to developing permselective membranes, research has focused on modifying working electrodes electrocatalytically to facilitate more efficient oxidation of NO. Fabricating NO sensors modified with Ni- and Co-phthalocyanines has been of particular interest based on their improved selectivity for NO (126,127). Of note, the conditions under which metallophthalocyanines are applied to electrodes greatly affect the analytical performance of the resulting sensor. Oni et al. sought to understand the influence of pH, temperature, solution ionic strength, and the type of ions present in solution on the performance of the resulting sensor (136). Co(II) phthalocyanine was deposited on glassy carbon electrodes by either electrodeposition or drop-casting. Differential pulse voltammetry data were then acquired using a 40 μM NO solution. While both electrode modification procedures reduced the potential required to generate an oxidation current, electrodeposition resulted in greater sensitivity (i.e., current) at a lower potential (~790 and ~900 mV versus Ag/AgCl reference for electrodeposition and drop-cast, respectively). It is likely that electrodeposition generates a more highly-ordered layer compared to drop-casting, facilitating the electron transfer process between adjacent Co(II) phthalocyanine molecules (136). The effect of changing the pH of the metallophthalocyanine deposition solution was also investigated. Ni(II) phthalocyanine tetrasulfonic acid tetrasodium salt deposited at pH 1, 4, 7, and 10 resulted in peak oxidation potentials for NO of 1040, 939, 822, and 868 mV (vs. Ag/AgCl), respectively. Deposition pH also affected the sensitivity of the sensor with the greatest peak current obtained from electrodes modified at pH 7. In a similar study, Hrbáč et al. optimized the conditions under which Ni(II) tetrakis(3-methoxy-4-hydroxyphenyl) porphyrin was deposited onto carbon fiber electrodes (129). The optimized membrane deposition procedure resulted in a NO sensor with a limit of detection of 1.5 nM and high selectivity over nitrite, ascorbate, and dopamine (129).

3.3. Other advances in electrochemical NO detection

The high affinity of NO for heme proteins has been coupled with electrochemical detection to create heme protein-based electrochemical NO sensors (137,138). For example, Fan et al. fabricated a hemoglobin-based NO biosensor that operated under aerobic conditions (137). A mixture of hemoglobin and sodium montmorillonite was cast on the surface of a polished pyrolytic graphite disk electrode. While the hemoglobin/montmorillonite film facilitated the reduction of oxygen, the addition of NO to the solution attenuated the O_2 reduction current, shifting the reduction potential more negative. The authors attributed this shift to competition between NO and O_2 for the heme site (137). Of analytical utility, the shift in potential was proportional to NO concentration. Furthermore, the sensor response to NO was linear to 5 μM NO with a limit of detection of 20 pM. With respect to interferents, both ascorbate and NO_2^- induced negligible peak shifts (<4% of that by the same concentration of NO), while dopamine, uric acid, and epinephrine proved to be significant interferents (shifts >15%) (137).

Although electrochemical sensors are both sensitive and fast responding, the development of sensors able to discriminate between NO and carbon monoxide (CO) still represents a critical need in the field of NO detection. Since NO and CO have similar properties (e.g., size, hydrophobicity, reactivity with heme proteins, oxidation potential, etc.), NO sensors traditionally possess little or no selectivity over CO. In fact, the literature commonly overlooks the selectivity over CO. To address this issue, Lee et al. developed an amperometric sensor for simultaneous detection of both NO and CO (139). To discriminate between NO and CO, a dual sensor was constructed with two working electrodes each having different sensitivities for NO and CO based on differences in electrode size and surface modification. Two Pt disk working electrodes (25 and 250 μm in diameter) were housed behind a PTFE gas-permeable membrane following their platinization. The larger electrode (250 μm) was further modified with an electrochemically deposited tin (Sn) layer to enhance its sensitivity to CO. This modification had a negligible effect on the NO response. When coupled, the two electrodes allowed for quantification of both NO and CO. The NO/CO sensor was characterized by limits of detection of ~1 and <5 nM for NO and CO, respectively, with linear responses up to μM levels for each analyte, and selectivity for NO and CO over ascorbic acid, uric acid, acetaminophen, and dopamine up to 500 μM and nitrite up to 1 mM. The authors employed the sensor to simultaneously monitor NO and CO in mice kidneys (ex vivo), and found that basal levels of CO production were ~7-fold greater than NO (139).

4. OTHER NO DETECTION TECHNIQUES

The spectroscopic and electrochemical methods described above are by far the most commonly-employed methods for measuring NO. Other less-frequently employed approaches include mass spectrometry (140,141), X-ray photoelectron spectroscopy (142), infrared (143–146) and UV (147–149) lasers, quartz crystal microbalance (150,151), photoluminescent porous silicon (152) and cadmium selenide (153), gas chromatography (154,155) and Raman spectroscopy (156). The scope of this review does not permit a detailed description of such detection techniques. However, it is important to note that these methods often consist of extensive instrumentation thus inhibiting throughput and analysis by non-experts.

Acknowledgments

M.H.S. acknowledges the National Institutes of Health (Grant EB000708) for support of his laboratory's sensor-related research.

LITERATURE CITED

1. Ignarro LJ, Buga GM, Wood KS, Byrns RE, Chaudhuri G. Endothelium-derived relaxing factor produced and released from artery and vein is nitric oxide. Proc. Natl. Acad. Sci. U.S.A. 1987; 84:9265–9269. [PubMed: 2827174]
2. Furchgott RF. Endothelium-derived relaxing factor: Discovery, early studies, and identification as nitric oxide (Nobel Lecture). Angew. Chem. Int. Ed. 1999; 38:1870–1880.
3. Loscalzo J, Welch G. Nitric oxide and its role in the cardiovascular system. Prog. Cardiovasc. Dis. 1995; 38:87–104. [PubMed: 7568906]
4. Bredt DS, Hwang PM, Snyder SH. Localization of nitric oxide synthase indicating a neural role for nitric oxide. Nature. 1990; 347:768–770. [PubMed: 1700301]
5. Shibuki K, Okada D. Endogenous nitric oxide release required for long-term synaptic depression in the cerebellum. Nature. 1991; 349:326–328. [PubMed: 1702879]
6. Fang FC. Mechanisms of nitric oxide-related antimicrobial activity. J. Clin. Invest. 1997; 99:2818–2825. [PubMed: 9185502]

7. Schwentker A, Vodovotz Y, Weller R, Billiar TR. Nitric oxide and wound repair: Role of cytokines? Nitric Oxide. 2002; 7:1–10. [PubMed: 12175813]
8. Bogdan C. Nitric oxide and the immune response. Nat. Immunol. 2001; 2:907–916. [PubMed: 11577346]
9. Luo JD, Chen AF. Nitric oxide: A newly discovered function on wound healing. Acta Pharm. Sinica. 2005; 26:259–264.
10. Moncada S, Higgs A. The L-arginine-nitric oxide pathway. N. Engl. J. Med. 1993; 329:2002–2012. [PubMed: 7504210]
11. Rosen GM, Tsai P, Pou S. Mechanism of free-radical generation by nitric oxide synthases. Chem. Rev. 2002; 102:1191–1199. [PubMed: 11942793]
12. Wang PG, Xian M, Tang X, Wu X, Wen Z, et al. Nitric oxide donors: Chemical activities and biological applications. Chem. Rev. 2002; 102:1091–1134. [PubMed: 11942788]
13. Hrabie JA, Keefer LK. Chemistry of the nitric oxide-releasing diazeniumdiolate ("nitrosohydroxylamine") functional group and its oxygen-substituted derivatives. Chem. Rev. 2002; 102:1135–1154. [PubMed: 11942789]
14. Wink DA, Mitchell JB. Chemical biology of nitric oxide: Insights into regulatory, cytotoxic, and cytoprotective mechanisms of nitric oxide. Free Radical Biol. Med. 1998; 25:434–456. [PubMed: 9741580]
15. Moller MN, Li Q, Lancaster JR, Denicola A. Acceleration of nitric oxide autoxidation and nitrosation by membranes. IUBMB Life. 2007; 59:243–248. [PubMed: 17505960]
16. Williams RJP. Nitric oxide in biology: Its role as a ligand. Chem. Soc. Rev. 1996; 25:77–83.
17. Girard P, Potier P. NO, thiols and disulfides. FEBS Lett. 1993; 320:7–8. [PubMed: 8462679]
18. Thomas DD, Ridnour LA, Espey MG, Donzelli S, Ambs S, et al. Superoxide fluxes limit nitric oxide-induced signaling. J. Biol. Chem. 2006; 281:25984–25993. [PubMed: 16829532]
19. Moritoshi S, Takahiro N, Mariko G, Yoshio U. Cell-based indicator to visualize picomolar dynamics of nitric oxide release from living cells. Anal. Chem. 2006; 78:8175–8182. [PubMed: 17165805]
20. Lancaster JR. A tutorial on the diffusibility and reactivity of free nitric oxide. Nitric Oxide. 1997; 1:18–30. [PubMed: 9701041]
21. Haussmann HJ, Werringloer J. Nitric oxide and nitrite formation during degradation of N-nitrosamines. Naunyn-Schmiedeberg's Arch. Pharmacol. 1985; 329:R21.
22. Noack E, Kubitzek D, Kojda G. Spectrophotometric determination of nitric oxide using hemoglobin. Neuroprotocols. 1992; 1:133–139.
23. Murphy ME, Noack E. Nitric oxide assay using hemoglobin method. Meth. Enzymol. 1994; 233:240–250. [PubMed: 8015461]
24. Doyle MP, Hoekstra JW. Oxidation of nitrogen oxides by bound dioxygen in hemeproteins. J. Inorg. Biochem. 1981; 14:351–358. [PubMed: 7276933]
25. Dacres H, Narayanaswamy R. A new optical sensing reaction for nitric oxide. Sens. Actuators, B. 2003; 90:222–229.
26. Kelm M, Freelisch M, Spahr R, Piper HM, Noack E, et al. Quantitative and kinetic characterization of nitric oxide and EDRF released from cultured endothelial cells. Biochem. Biophys. Res. Comm. 1988; 154:236–244. [PubMed: 3260776]
27. Zhou Q, Hellermann GR, Solomonson LP. Nitric oxide release from resting human platelets. Thrombosis Res. 1995; 77:87–96.
28. Kelm M, Schrader J. Nitric oxide release from the isolated guinea pig heart. Eur. J. Pharmacol. 1988; 155:317–321. [PubMed: 3234489]
29. Zhang Y, Samson FE, Nelson SR, Pazdernik TL. Nitric oxide detection with intracerebral microdialysis: Important considerations in the application of the hemoglobin-trapping technique. J. Neurosci. Meth. 1996; 68:165–173.
30. Boon EM, Marletta MA. Sensitive and selective detection of nitric oxide using an H-NOX domain. J. Am. Chem. Soc. 2006; 128:10022–10023. [PubMed: 16881625]
31. Aylott JW, Richardson DJ, Russell DA. Optical biosensing of gaseous nitric oxide using spin-coated sol-gel thin films. Chem. Mater. 1997; 9:2261–2263.

32. Lan EH, Dave BC, Fukuto JM, Dunn B, Zink JI, et al. Synthesis of sol-gel encapsulated heme proteins with chemical sensing properties. J. Mater. Chem. 1999; 9:45–53.
33. Bull C, Fisher RG, Hoffman BM. Manganese hemoglobin: Allosteric effects in redox and ligation equilibria. Biochem. Biophys. Res. Comm. 1974; 59:140–145. [PubMed: 4858350]
34. Dacres H, Narayanaswamy R. Sensitive optical NO sensor based on bis [(2,9-dimethyl-1,10-phenanthroline)] copper(II) complex. Sens. Actuators, B. 2005; 107:14–23.
35. Dacres H, Narayanaswamy R. Evaluation of copper(II) eriochrome cyanine R (ECR) complex immobilized in anion exchange membrane as a potential nitric oxide optical sensor. Aust. J. Chem. 2008; 61:189–196.
36. Griess JP. On a new series of bodies in which nitrogen is substituted for hydrogen. Philos. Trans. R. Soc. (London). 1864; 154:667–731.
37. Sun J, Zhang X, Broderick M, Fein H. Measurement of nitric oxide production in biological systems by using Griess reaction assay. Sensors. 2003; 3:276–284.
38. Tsikas D. Analysis of nitrite and nitrate in biological fluids by assays based on the Griess reaction: Appraisal of the Griess reaction in the L-arginine/nitric oxide area of research. J. Chromatogr. B. 2007; 851:51–70.
39. Bratton AC, Marshall EK. A new coupling component for sulfanilamide determination. J. Biol. Chem. 1939; 128:537–550.
40. Tracey WR. Spectrophotometric detection of nitrogen oxides using azo dyes. Neuroprotocols. 1992; 1:125–131.
41. Granger DL, Taintor RR, Boockvar KS, Hibbs JB. Measurement of nitrate and nitrite in biological samples using nitrate reductase and Griess reaction. Methods Enzymol. 1996; 268:142–151. [PubMed: 8782580]
42. Verdon CP, Burton BA, Prior RL. Sample pretreatment with nitrate reductase and glucose-6-phosphate dehydrogenase quantitatively reduces nitrate while avoiding interference by $NADP^+$ when the Griess reaction is used to assay for nitrite. Anal. Biochem. 1995; 224:502–508. [PubMed: 7733451]
43. Joharchi K, Jorjani M. The role of nitric oxide in diabetes-induced changes of morphine tolerance in rats. Eur. J. Pharmacol. 2007; 570:66–71. [PubMed: 17599829]
44. Keles MS, Taysi S, Aksoy H, Sen N, Polat F, et al. The effect of corticosteroids on serum and cerebrospinal fluid nitric oxide levels in multiple sclerosis. Clin. Chem. Lab. Med. 2001; 39:827–820. [PubMed: 11601681]
45. Giustarini D, Dalle-Donne I, Colombo R, Milzani A, Rossi R. Adaptation of the Griess reaction for detection of nitrite in human plasma. Free Radical Res. 2004; 38:1235–1240. [PubMed: 15621701]
46. Ozkan Y, Yardim-Akaydin S, Sepici A, Engin B, Sepici V, et al. Assessment of homocysteine, neopterin and nitric oxide levels in Behcet's disease. Clin. Chem. Lab. Med. 2007; 45:73–77. [PubMed: 17243919]
47. Schulz K, Kerber S, Kelm M. Reevaluation of the Griess method for determining NO/NO_2^- in aqueous and protein-containing samples. Nitric Oxide. 1999; 3:225–234. [PubMed: 10442854]
48. Ullrich T, Oberle S, Abate A, Schroder H. Photoactivation of the nitric oxide donor SIN-1. FEBS Lett. 1997; 406:66–68. [PubMed: 9109387]
49. Klink M, Cedzynski M, Swierzko A, Tchorzewski H, Sulowska Z. Involvement of nitric oxide donor compounds in the bactericidal activity of human neutrophils in vitro. J. Med. Microbiol. 2003; 52:303–308. [PubMed: 12676868]
50. Taite LJ, West JL. Poly(ethylene glycol)-lysine dendrimers for targeted delivery of nitric oxide. J. Biomater. Sci. Polymer Edn. 2006; 17:1159–1172.
51. Kapadia MR, Chow LW, Tsihlis ND, Ahanchi SS, Eng JW, et al. Nitric oxide and nanotechnology: A novel approach to inhibit neointimal hyperplasia. J. Vasc. Surg. 2008; 47:173–182. [PubMed: 18178471]
52. Ohta T, Goto N, Takitani S. Spectrophotometric determination of *N*-nitroso compounds by flow injection analysis. Analyst. 1988; 113:1333–1335. [PubMed: 3232841]

53. Hirata S, Amma BV, Karthikeyan S, Toda K. Determination of nitrite by flow injection spectrophotometry using a home-made flow cell detector. Anal. Sci. 2003; 19:1687–1689. [PubMed: 14696939]
54. Higuchi K, Motomizu S. Flow-injection spectrophotometric determination of nitrite and nitrate in biological samples. Anal. Sci. 1999; 15:129–134.
55. Toda K, Hato Y, Ohira SI, Namihira T. Micro-gas analysis system for measurement of nitric oxide and nitrogen dioxide: Respiratory treatment and environmental mobile monitoring. Anal. Chim. Acta. 2007; 603:60–66. [PubMed: 17950058]
56. Gomes A, Fernandes E, Lima JLFC. Use of fluorescence probes for detection of reactive nitrogen species: A review. J. Fluoresc. 2006; 16:119–139. [PubMed: 16477509]
57. Meineke P, Rauen U, de Groot H, Koth HG. Cheletropic traps for the fluorescence spectroscopic detection of nitric oxide (nitrogen monoxide) in biological systems. Chem. A Eur. J. 1999; 5:1738–1747.
58. Meineke P, Rauen U, de Groot H, Korth HG, Sustmann R. Nitric oxide detection and visualization in biological systems. Applications of the FNOCT method. Biol. Chem. 2000; 381:575–582. [PubMed: 10987364]
59. Lim MH, Lippard SJ. Metal-based turn-on fluorescent probes for sensing nitric oxide. Acc. Chem. Res. 2007; 40:41–51. [PubMed: 17226944]
60. Lim MH, Wong BA, Pitcock WH, Mokshagundam D, Baik MH, et al. Direct nitric oxide detection in aqueous solution by copper(II) fluorescein complexes. J. Am. Chem. Soc. 2006; 128:14364–14373. [PubMed: 17076510]
61. Lim MH, Xu D, Lippard SJ. Visualization of nitric oxide in living cells by a copper-based fluorescent probe. Nat. Chem. Biol. 2006; 2:375–380. [PubMed: 16732295]
62. Kojima H, Sakurai K, Kikuchi K, Kawahara S, Kirino Y, et al. Development of a fluorescent indicator for nitric oxide based on the fluorescein chromophore. Chem. Pharm. Bull. 1998; 46:373–375. [PubMed: 9501473]
63. Kojima H, Kakatsubo N, Kikuchi K, Kawahara S, Kirino Y, et al. Detection and imaging of nitric oxide with novel fluorescent indicators: Diaminofluoresceins. Anal. Chem. 1998; 70:2446–2453. [PubMed: 9666719]
64. Patel VH, Brack KE, Coote JH. A novel method of measuring nitric-oxide-dependent fluorescence using 4,5-diaminofluorescein (DAF-2) in the isolated Langendorff-perfused rabbit heart. Pflugers Arch. Eur. J. Physiol. 2008; 456:635–645. [PubMed: 18180949]
65. Lepiller S, Laurens V, Bouchot A, Herbomel P, Solary E, et al. Imaging of nitric oxide in a living vertebrate using a diaminofluorescein probe. Free Radical Biol. Med. 2007; 43:619–627. [PubMed: 17640572]
66. Strijdom H, Muller C, Lochner A. Direct intracellular nitric oxide detection in isolated adult cardiomyocytes: Flow cytometric analysis using the fluorescent probe, diaminofluorescein. J. Mol. Cell Cardiol. 2004; 37:897–902. [PubMed: 15380680]
67. Havenga MJE, van Dam V, Groot BS, Grimbergen JM, Valerio D, et al. Simultaneous detection of NOS-3 protein expression and nitric oxide production using a flow cytometer. Anal. Biochem. 2001; 290:283–291. [PubMed: 11237331]
68. Ward TR, Mundy WR. Measurement of nitric oxide synthase activity using the citrulline assay. Methods Mol. Med. 1999; 22:157–162. [PubMed: 21380831]
69. Huang KJ, Wang H, Zhang QY, Ma M, Hu JF, et al. Direct detection of nitric oxide in human blood serum by use of 1,3,5,7-tetramethyl-8-(3',4'-diaminophenyl) difluoroboradiaza-*s*-indacene with HPLC. Anal. Bioanal. Chem. 2006; 384:1284–1290. [PubMed: 16496132]
70. Huang KJ, Zhang M, Xie WZ, Zhang HS, Feng YQ, et al. Sensitive determination of nitric oxide in some rat tissues using polymer monolith microextraction coupled to high-performance liquid chromatography with fluorescence detection. Anal. Bioanal. Chem. 2007; 388:939–946. [PubMed: 17447053]
71. Kim WS, Ye X, Rubakhin SS, Sweedler JV. Measuring nitric oxide in single neurons by capillary electrophoresis with laser-induced fluorescence: Use of ascorbate oxidase in diaminofluorescein measurements. Anal. Chem. 2006; 78:1859–1865. [PubMed: 16536421]

72. Zhang X, Kim WS, Hatcher N, Potgieter K, Moroz LL, et al. Interfering with nitric oxide measurements. J. Biol. Chem. 2002; 277:48472–48478. [PubMed: 12370177]
73. Barker SLR, Kopelman R, Meyer TE, Cusanovich MA. Fiber-optic nitric oxide-selective biosensors and nanosensors. Anal. Chem. 1998; 70:971–976. [PubMed: 9511472]
74. Barker SLR, Kopelman R. Development and cellular applications of fiber optic nitric oxide sensors based on a gold-adsorbed fluorophore. Anal. Chem. 1998; 70:4902–4906. [PubMed: 9852778]
75. Barker SLR, Clark HA, Swallen SF, Kopelman R, Tsang AW, et al. Ratiometric and fluorescence-lifetime-based biosensors incorporating cytochrome *c*′ and the detection of extra- and intracellular macrophage nitric oxide. Anal. Chem. 1999; 71:1767–1772. [PubMed: 10330907]
76. Bates JN. Nitric oxide measurement by chemiluminescence detection. Neuroprotocols. 1992; 1:141–149.
77. GE Sievers Nitric Oxide Analyzer (NOA 280i) Fact Sheet. 2008 http://www.geinstruments.com/ionics/SearchableFiles/Library/Brochures/NotProtected/NOA_280i_brochure.pdf.
78. Shin JH, Schoenfisch MH. Inorganic/organic hybrid silica nanoparticles as a nitric oxide delivery scaffold. Chem. Mater. 2008; 20:239–249.
79. Stasko NA, Fischer TH, Schoenfisch MH. *S*-Nitrosothiol-modified dendrimers as nitric oxide delivery vehicles. Biomacromolecules. 2008; 9:834–841. [PubMed: 18247567]
80. Marxer SM, Rothrock AR, Nablo BJ, Robbins ME, Schoenfisch MH. Preparation of nitric oxide (NO)-releasing sol-gels for biomaterial applications. Chem. Mater. 2003; 15:4193–4199.
81. Nowicki PT, Caniano DA, Hammond S, Giannone PJ, Besner GE, et al. Endothelial nitric oxide synthase in human intestine resected for necrotizing enterocolitis. J. Pediatr. 2007; 150:40–45. [PubMed: 17188611]
82. Tsang KW, Ip SK, Leung R, Tipoe GL, Chan SL, et al. Exhaled nitric oxide: The effects of age, gender and body size. Lung. 2001; 179:83–91. [PubMed: 11733851]
83. Kikuchi K, Nagano T, Hayakawa H, Hirata Y, Hirobe M. Detection of nitric oxide production from a perfused organ by a luminol-H_2O_2 system. Anal. Chem. 1993; 65:1794–1799. [PubMed: 8368532]
84. Robinson JK, Bollinger MJ, Birks JW. Luminol/H_2O_2 chemiluminescence detector for the analysis of nitric oxide in exhaled breath. Anal. Chem. 1999; 71:5131–5136. [PubMed: 10575964]
85. Zhou X, Arnold MA. Response characteristics and mathematical modeling for a nitric oxide fiber-optic chemical sensor. Anal. Chem. 1996; 68:1748–1754.
86. Kleschyov AL, Wenzel P, Munzel T. Electron paramagnetic resonance (EPR) spin trapping of biological nitric oxide. J. Chromatogr., B. 2007; 851:12–20.
87. Dikalov S, Fink B. ESR techniques for the detection of nitric oxide in vivo and in tissues. Methods Enzymol. 2005; 396:597–610. [PubMed: 16291267]
88. Hall DM, Buettner GR, Gisolfi CV. In vivo detection of nitric oxide and NO_x species using ex vivo electron paramagnetic resonance spectroscopy. Microchem. J. 1997; 56:165–170.
89. Van Doorslaer S, Desmet F. The power of using continuous-wave and pulsed electron paramagnetic resonance methods for the structure analysis of ferric forms and nitric oxide-ligated ferrous forms of globins. Methods Enzymol. 2008; 437:287–310. [PubMed: 18433634]
90. Kuppusamy P, Shankar RA, Roubaud VM, Zweier JL. Whole body detection and imaging of nitric oxide generation in mice following cardiopulmonary arrest: Detection of intrinsic nitrosoheme complexes. Magn. Reson. Med. 2001; 45:700–707. [PubMed: 11283999]
91. Vanin AF, Poltorakov AP, Mikoyan VD, Kubrina LN, van Faassen E. Why iron-dithiocarbamates ensure detection of nitric oxide in cells and tissues. Nitric Oxide. 2006; 15:295–311. [PubMed: 16403659]
92. Pustelny K, Bielanska J, Plonka PM, Rosen GM, Elas M. In vivo spin trapping of nitric oxide from animal tumors. Nitric Oxide. 2007; 16:202–208. [PubMed: 17113795]
93. Ren J, Fung PCW, Chang C, Shen GX, Lu G, et al. A comparative ESR study on blood and tissue nitric oxide concentration during renal ischemia-reperfusion injury. Appl. Magn. Reson. 2007; 32:243–255.

94. Quaresima V, Takehara H, Tsushima K, Ferrari M, Utsumi H. In vivo detection of mouse liver nitric oxide generation by spin trapping electron paramagnetic resonance spectroscopy. Biochem. Biophys. Res. Comm. 1996; 221:729–734. [PubMed: 8630029]
95. Komarov AM. In vivo detection of nitric oxide distribution in mice. Molec. Cell. Biochem. 2002; 234/235:387–392. [PubMed: 12162457]
96. Xu YC, Cao YL, Guo P, Tao Y, Zhao BL. Detection of nitric oxide in plants by electron spin resonance. Phytopathology. 2004; 94:402–407. [PubMed: 18944117]
97. Hirayama A, Nagase S, Ueda A, Yoh K, Oteki T, et al. Electron paramagnetic resonance imaging of nitric oxide organ distribution in lipopolysuccaride treated mice. Molec. Cell. Biochem. 2003; 244:63–67. [PubMed: 12701811]
98. Vanin AF, Huisman A, van Faassen EE. Iron dithiocarbamate as spin trap for nitric oxide detection: pitfalls and successes. Methods Enzymol. 2002; 359:27–42. [PubMed: 12481557]
99. Vanin AF. Iron diethyldithiocarbamate as spin trap for nitric oxide detection. Methods Enzymol. 1999; 301:269–279. [PubMed: 9919576]
100. Fujii S, Yoshimura T, Kamada H. Nitric oxide trapping efficiencies of water-soluble iron(III) complexes with dithiocarbamate derivatives. Chem. Lett. 1996; 25:785–786.
101. Yoshimura T, Fujii S, Yokoyama H, Kamada H. In vivo electron paramagnetic resonance imaging of NO-bound iron complex in a rat head. Chem. Lett. 1995; 24:309–310.
102. Yoshimura T, Yokoyama H, Fujii S, Takayama F, Oikawa K, et al. In vivo EPR detection and imaging of endogenous nitric oxide in lipopolysaccharide-treated mice. Nature Biotech. 1996; 14:992–994.
103. Nakagawa H, Ikota N, Ozawa T, Masumizu T, Kohno M. Spin trapping for nitric oxide produced in LPS-treated mouse using various new dithiocarbamate iron complexes having substituted proline and serine moiety. Biochem. Mol. Bio. Int. 1998; 45:1129–1138. [PubMed: 9762411]
104. Paschenko SV, Khramtsov VV, Skatchkov MP, Plyusnin VF, Bassenge E. EPR and laser flash photolysis studies of the reaction of nitric oxide with water soluble NO trap Fe(II)-proline dithiocarbamate complex. Biochem. Biophys. Res. Comm. 1996; 225:557–584. [PubMed: 8753800]
105. Weaver J, Porasuphatana S, Tsai P, Budzichowski T, Rosen GM. Spin trapping nitric oxide from neuronal nitric oxide synthase: A look at several iron-dithiocarbamate complexes. Free Radical Res. 2005; 39:1027–1033. [PubMed: 16298728]
106. Kleschyov AL, Muller B, Keravis T, Stoeckel ME, Stoclet JC. Adventitia-derived nitric oxide in rat aortas exposed to endotoxin: Cell origin and functional consequences. Am. J. Physiol. Heart Circ. Physiol. 2000; 279:H2743–H2751. [PubMed: 11087229]
107. Ciszewski A, Milczarek G. Electrochemical detection of nitric oxide using polymer modified electrodes. Talanta. 2003; 61:11–26. [PubMed: 18969158]
108. Malinski T, Taha Z. Nitric oxide release from a single cell measured in situ by a porphyrinic-based microsensor. Nature. 1992; 358:676–678. [PubMed: 1495562]
109. Malinski T, Taha Z, Grunfeld S, Burewicz A, Tomboulian P, et al. Measurements of nitric oxide in biological materials using a porphyrinic microsensor. Anal. Chim. Acta. 1993; 279:135–140.
110. Maskus M, Pariente F, Wu Q, Toffanin A, Shapleigh JP, et al. Electrocatalytic reduction of nitric oxide at electrodes modified with electropolymerized films of $[Cr(v\text{-}tpy)_2]^{3+}$ and their application to cellular NO determinations. Anal. Chem. 1996; 68:3128–3134. [PubMed: 8797375]
111. Fan C, Li G, Zhu J, Zhu D. A reagentless nitric oxide biosensor based on hemoglobin-DNA films. Anal. Chim. Acta. 2000; 423:95–100.
112. Zen J, Kumar AS, Wang H. A dual electrochemical sensor for nitrite and nitric oxide. Analyst. 2000; 125:2169–2172. [PubMed: 11219047]
113. Fan C, Pang J, Shen P, Li G, Zhu D. Nitric oxide biosensors based on Hb/phosphatidylcholine films. Anal. Sci. 2002; 18:129–132. [PubMed: 11874112]
114. Christodoulou D, Kudo S, Cook JA, Krishna MC, Miles A, et al. Electrochemical methods for detection of nitric oxide. Methods Enzymol. 1996; 268:69–83. [PubMed: 8782574]
115. Shin JH, Weinman S, Schoenfisch MH. Sol-gel derived amperometric nitric oxide microsensor. Anal. Chem. 2005; 77:3494–3501. [PubMed: 15924380]

116. Shibuki K. An electrochemical microprobe for detecting nitric oxide release in brain tissue. Neurosci. Res. 1990; 9:69–76. [PubMed: 2175870]
117. Cserey A, Gratzl M. Stationary-state oxidized platinum microsensor for selective and on-line monitoring of nitric oxide in biological preparations. Anal. Chem. 2001; 73:3965–3974. [PubMed: 11534724]
118. Kitamura Y, Uzawa T, Oka K, Komai Y, Takizawa N, et al. Microcoaxial electrode for in vivo nitric oxide measurement. Anal. Chem. 2000; 72:2957–2962. [PubMed: 10905334]
119. Prakash R, Srivastava RC, Seth PK. polycarbazole modified electrode; nitric oxide sensor. Polym. Bull. 2001; 46:487–490.
120. Kashevskii AV, Safronov AY, Ikeda O. Behaviors of H_2TPP and CoTPPCl in Nafion film and the catalytic activity for nitric oxide oxidation. J. Electroanal. Chem. 2001; 510:86–95.
121. Ciszewski A, Milczarek G. Preparation and general properties of chemically modified electrodes based on electrosynthesized thin polymeric films derived from eugenol. Electroanalysis. 2001; 13:860–867.
122. Kato D, Sakata M, Hirayama C, Hirata Y, Mizutani F, et al. Selective permeation of nitric oxide through two dimensional cross-linked polysiloxane LB films. Chem. Lett. 2002; 31:1190–1191.
123. Do JS, Wu KJ, Tsai ML. Amperometric NO gas sensor in the presence of diffusion barrier: Selectivity, mass transfer of NO and effect of temperature. Sens. Actuators, B. 2002; 86:98–105.
124. Park JK, Tran PH, Chao JKT, Ghodadra R, Rangarajan R, et al. In vivo nitric oxide sensor using non-conducting polymer-modified carbon fiber. Biosens. Bioelectron. 1998; 13:1187–1195. [PubMed: 9871974]
125. Diab N, Schuhmann W. Electropolymerized manganese porphyrin/polypyrrole films as catalytic surfaces for the oxidation of nitric oxide. Electrochim. Acta. 2001; 47:265–273.
126. Pontie M, Gobin C, Pauporte T, Bedioui F, Devynck J. Electrochemical nitric oxide microsensors: Sensitivity and selectivity characterization. Anal. Chim. Acta. 2000; 411:175–185.
127. Pereira-Rodrigues N, Albin V, Koudelka-Hep M, Auger V, Pailleret A, et al. Nickel tetrasulfonated phthalocyanine based platinum microelectrode array for nitric oxide oxidation. Electrochem. Comm. 2002; 4:922–927.
128. Casero E, Pariente F, Lorenzo E, Beyer L, Losada J. Electrocatalytic oxidation of nitric oxide at 6,17-Diferrocenyl-dibenzo[b,i]5,9,14,18-tetraaza[14]annulen]-nickel(II) modified electrodes. Electroanalysis. 2001; 13:1411–1416.
129. Hrbac J, Gregor C, Machova M, Kralova J, Bystron T, et al. Nitric oxide sensor based on carbon fiber covered with nickel porphyrin layer deposited using optimized electropolymerization procedure. Bioelectrochem. 2007; 71:46–53.
130. Mao L, Yamamoto K, Zhou W, Jin L. Electrochemical nitric oxide sensors based on electropolymerized film of M(salen) with central ions of Fe, Co, Cu, and Mn. Electroanalysis. 2000; 12:72–77.
131. Bedioui F, Villeneuve N. Electrochemical nitric oxide sensors for biological samples - principle, selected examples and applications. Electroanalysis. 2003; 15:5–18.
132. Lee Y, Oh BK, Meyerhoff ME. Improved planar amperometric nitric oxide sensor based on platinized platinum anode. 1. Experimental results and theory when applied for monitoring NO release from diazeniumdiolate-doped polymeric films. Anal. Chem. 2004; 76:536–544. [PubMed: 14750844]
133. Feltham AM, Spiro M. Platinized platinum electrodes. Chem. Rev. 1971; 71:177–193.
134. Cha W, Meyerhoff ME. Enhancing the selectivity of amperometric nitric oxide sensor over ammonia and nitrite by modifying gas-permeable membrane with Teflon AF. Chem. Anal. 2006; 949:949–961.
135. Shin JH, Privett BJ, Kita JM, Wightmant RM, Schoenfisch MH. Fluorinated xerogel-derived ultramicroelectrodes for amperometric nitric oxide sensing. Anal. Chem. 2008 in press.
136. Oni J, Diab N, Reiter S, Schuhmann W. Metallophthalocyanine-modified glassy carbon electrodes: Effects on film formation conditions on electrocatalytic activity towards the oxidation of nitric oxide. Sens. Actuators, B. 2005; 105:208–213.
137. Fan C, Liu X, Pang J, Li G, Scheer H. Highly sensitive voltammetric biosensor for nitric oxide based on its high affinity with hemoglobin. Anal. Chim. Acta. 2004; 523:225–228.

138. Guo Z, Chen J, Liu H, Cha C. Direct electrochemistry of hemoglobin and myoglobin at didodecyldimethylammonium bromide-modified powder microelectrode and application for electrochemical detection of nitric oxide. Anal. Chim. Acta. 2008; 607:30–36. [PubMed: 18155406]
139. Lee Y, Kim J. Simultaneous electrochemical detection of nitric oxide and carbon monoxide generated from mouse kidney organ tissues. Anal. Chem. 2007; 79:7669–7675. [PubMed: 17877421]
140. Conrath U, Amoroso G, Kohle H, Sultemeyer DF. Non-invasive online detection of nitric oxide from plants and some other organisms by mass spectrometry. The Plant Journal. 2004; 38:1015–1022. [PubMed: 15165192]
141. Bethke PC, Badger MR, Jones RL. Apoplastic synthesis of nitric oxide by plant tissues. The Plant Cell. 2004; 16:332–341. [PubMed: 14742874]
142. Dubey M, Bernasek SL, Schwartz J. Highly sensitive nitric oxide detection using X-ray photoelectron spectroscopy. J. Am. Chem. Soc. 2007; 129:6980–6981. [PubMed: 17497778]
143. Nelson DD, Shorter JH, McManus JB, Zahniser MS. Sub-part-per-billion detection of nitric oxide in air using a thermoelectrically cooled mid-infrared quantum cascade laser spectrometer. Appl. Phys. B. 2002; 75:343–350.
144. Bakhirkin YA, Kosterev AA, Roller C, Curl RF, Tittel FK. Mid-infrared quantum cascade laser based off-axis integrated cavity output spectroscopy for biogenic nitric oxide detection. Appl. Optics. 2004; 43:2257–2266.
145. McManus JB, Nelson DD, Herndon SC, Shorter JH, Zahniser MS, et al. Comparison of cw and pulsed operation with a TE-cooled quantum cascade infrared laser for detection of nitric oxide at 1900 cm^{-1}. Appl. Phys. B. 2006; 85:235–241.
146. Grossel A, Zeninari V, Joly L, Parvitte B, Durry G, et al. Photoacoustic detection of nitric oxide with a Helmholtz resonant quantum cascade laser sensor. Infrared Phys. Tech. 2007; 51:95–101.
147. Reeves M, Farrell PV, Musculus MP. Demonstration of a two-photon, confocal laser-induced fluorescence technique for the detection of nitric oxide in atmospheric pressure flows and hydrocarbon-air flames. Meas. Sci. Technol. 1999; 10:285–294.
148. Dilecce G, Ambrico PF, Simek M, De Benedictis S. New laser-induced fluorescence scheme for simultaneous OH and NO detection by a single laser set-up. Appl. Phys. B. 2002; 75:131–135.
149. Bloss WJ, Gravestock TJ, Heard DE, Ingham T, Johnson GP, et al. Application of a compact all solid-state laser system to the in situ detection of atmospheric OH, HO_2, NO and IO by laser-induced fluorescence. J. Environ. Monit. 2003; 5:21–28. [PubMed: 12619752]
150. Zhang J, Hu J, Zhu ZQ, Gong H, O'Shea SJ. Quartz crystal microbalance coated with sol-gel-derived indium-tin oxide thin films as gas sensor for NO detection. Colloids Surf., A. 2004; 236:23–30.
151. Zhang J, Hu JQ, Zhu FR, Gong H, O'Shea SJ. ITO thin films coated quartz crystal microbalance as gas sensor for NO detection. Sens. Actuators, B. 2002; 87:159–167.
152. Harper J, Sailor MJ. Detection of nitric oxide and nitrogen dioxide with photoluminescent porous silicon. Anal. Chem. 1996; 68:3713–3717. [PubMed: 21619242]
153. Ivanisevic A, Reynolds MF, Burstyn JN, Ellis AB. Photoluminescent properties of cadmium selenide in contact with solutions and films of metalloporphyrins: Nitric oxide sensing and evidence for the aversion of an analyte to a buried semiconductor-film interface. J. Am. Chem. Soc. 2000; 122:3731–3738.
154. Funazo K, Tanaka M, Shono T. Gas chromatographic determination of nitric oxide at sub-ppm levels. Anal. Chim. Acta. 1980; 119:291–297.
155. Pai T, Payne W, LeGall J. Use of a chemiluminescence detector for quantitation of nitric oxide produced in assays of denitrifying enzymes. Analyt. Biochem. 1987; 166:150–157. [PubMed: 3674405]
156. Doerk T, Ehlbeck J, Jedamzik R, Uhlenbusch J, Hoschele J, et al. Application of coherent anti-Stokes Raman scattering (CARS) technique to the detection of NO. Appl. Spectrosc. 1997; 51:1360–1368.

SUMMARY POINTS

1. Detection of nitric oxide (NO) presents unique challenges to analytical chemists due to its rapid scavenging, high reactivity, swift diffusion, and wide range of physiologically-relevant concentrations.
2. The most commonly employed methods for measuring NO are based on spectroscopy and electrochemistry.
3. Absorbance-based methods (e.g., metalloprotein-based assays, Griess reaction) benefit from simple instrumentation and experimental procedures, but suffer from the inability to detect NO in real-time and at low concentrations.
4. Common NO-sensitive fluorescent probes are usually sensitive to a reactive byproduct of NO oxidation (e.g., N_2O_3).
5. The two types of chemiluminescent reactions that exist for NO detection are based on NO or a byproduct reacting with ozone or luminol; both have low limits of detection (fM – nM) and wide detection ranges (up to 6 orders of magnitude).
6. Electron paramagnetic resonance spectroscopy coupled with both endogenous and exogenous NO spin traps provides a useful method for detecting and imaging NO production in biological samples both in vivo and ex vivo.
7. Sensitive and selective electrochemical NO sensors have been fabricated using permselective sensor membranes and/or electrocatalytic sensor modifications to reduce the potential necessary to oxidize NO.
8. The major challenge for electrochemical NO sensors is reducing the signal generated by common interferents such as oxygen, nitrite, ascorbic acid, uric acid, dopamine, and carbon monoxide.

FUTURE ISSUES

1. Future research should focus on methods to correlate intracellular fluorescence from NO-sensitive fluorescent probes to an actual concentration of NO. Achieving this would likely require coupling several analytical approaches such as NO-sensitive fluorescent probes, confocal microscopy, and electrochemical NO measurements.
2. Carbon monoxide continues to pose a significant problem as an interferent for NO detection. Techniques for better discriminating between NO and CO are still required, especially for electrochemical sensors.
3. Sensors capable of measuring NO simultaneously in all its forms, including reactive nitrogen oxide (rNO_x) species (e.g., NO, NO_2, N_2O_3, N_2O_4, $ONOO^-$), nitrosothiols, and metal-NO complexes, represent an attribute that would improve the understanding of NO's role in physiology.

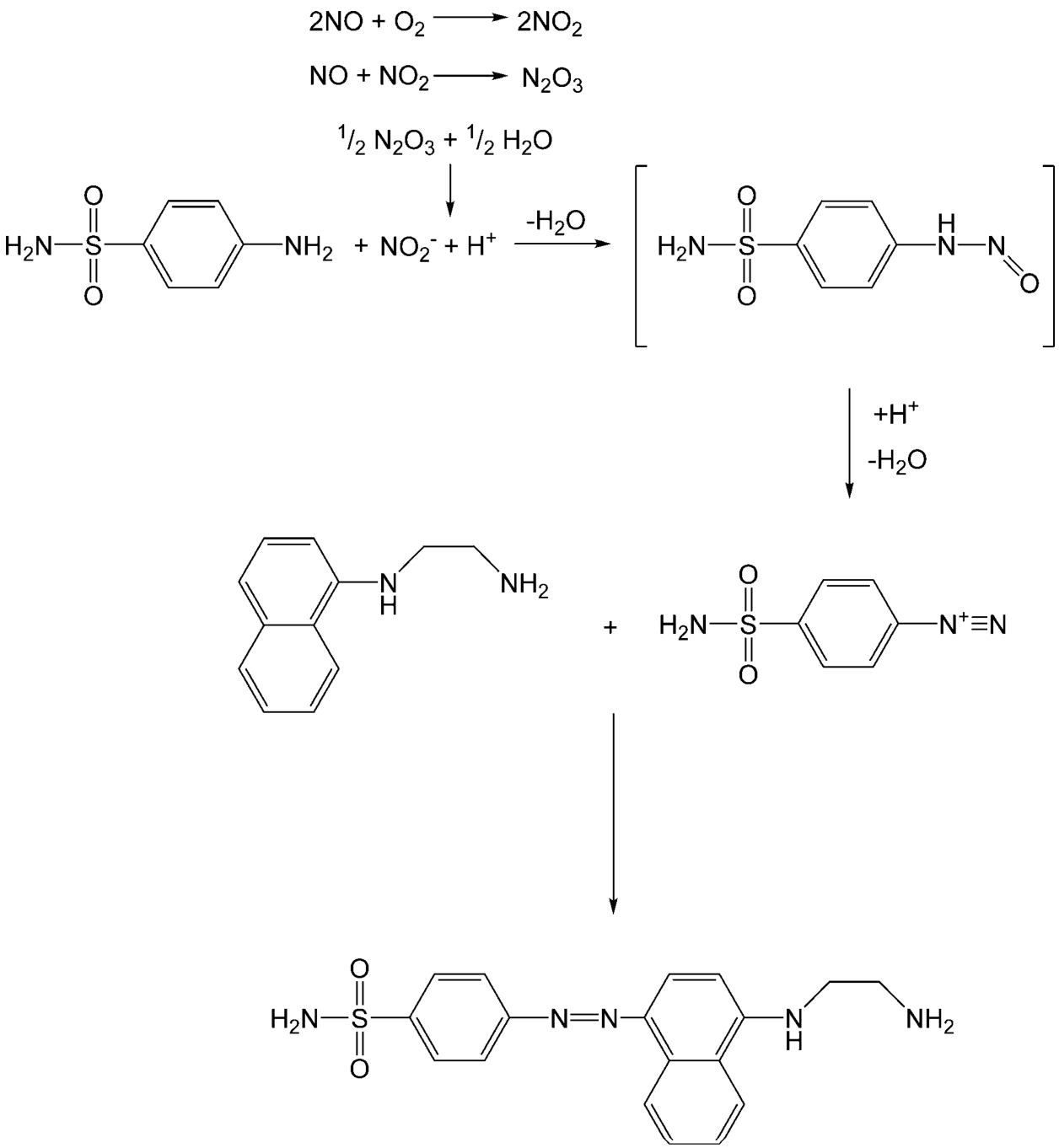

Figure 1.
The most commonly employed diazotization reaction (Griess assay). Under aerobic conditions nitric oxide (NO) reacts to form nitrite (NO_2^-), which reacts with sulfanilic acid to form a diazonium salt intermediate. The diazonium salt is then coupled to *N*-(1-naphthyl)ethylenediamine to form the stable water-soluble azo dye ($\lambda_{max} \approx 540$ nm).

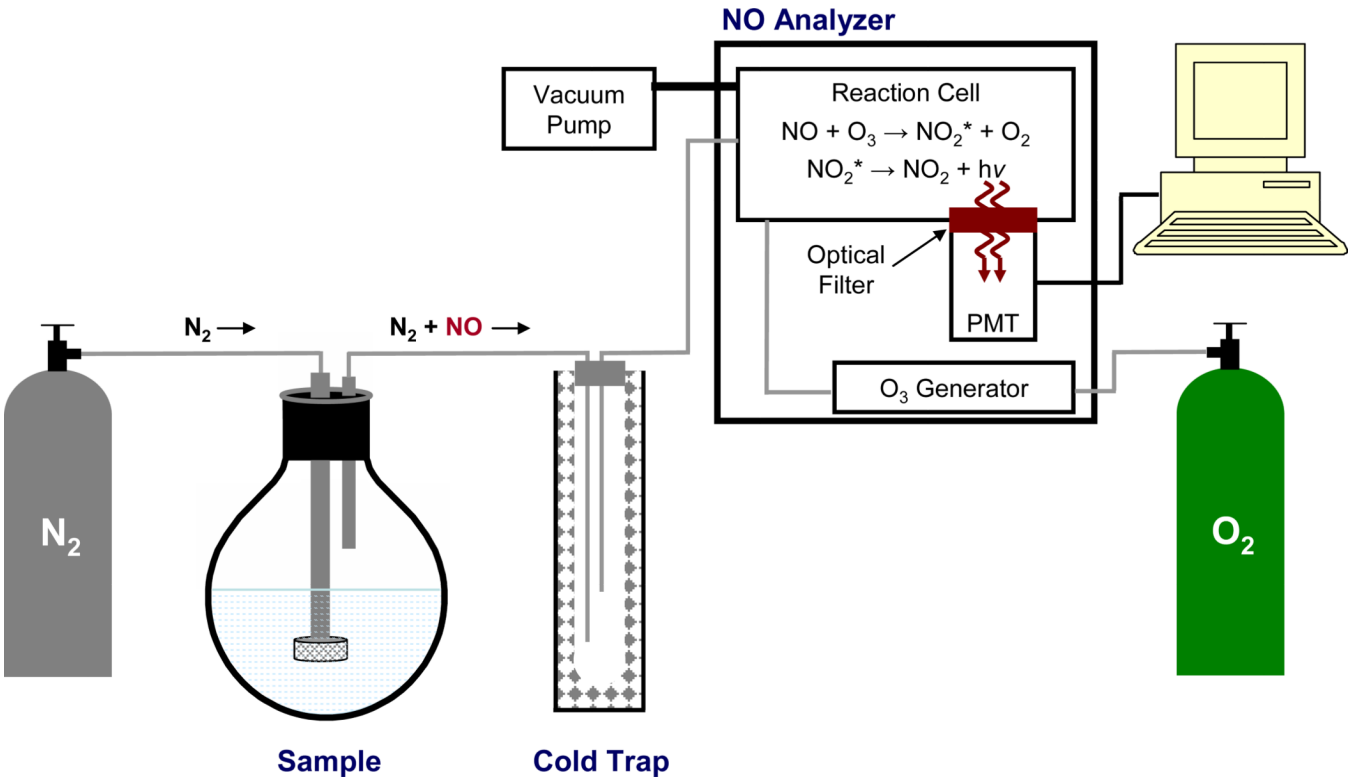

Figure 2.
Schematic diagram of a chemiluminescence-based nitric oxide analyzer. An intert gas (e.g., nitrogen (N_2)) is used to both deoxygenate sample buffer and carry NO from the sample flask though a cold trap (to remove water vapor) into a reaction cell within the nitric oxide analyzer. In the reaction cell, nitric oxide (NO) reacts with ozone (O_3) to form excited-state nitrogen dioxide (NO_2*), which emits a photon (i.e., chemiluminescence) upon its relaxation to the ground state (NO_2). Emitted light passes through an optical filter and is detected by a photomultiplier tube (PMT).

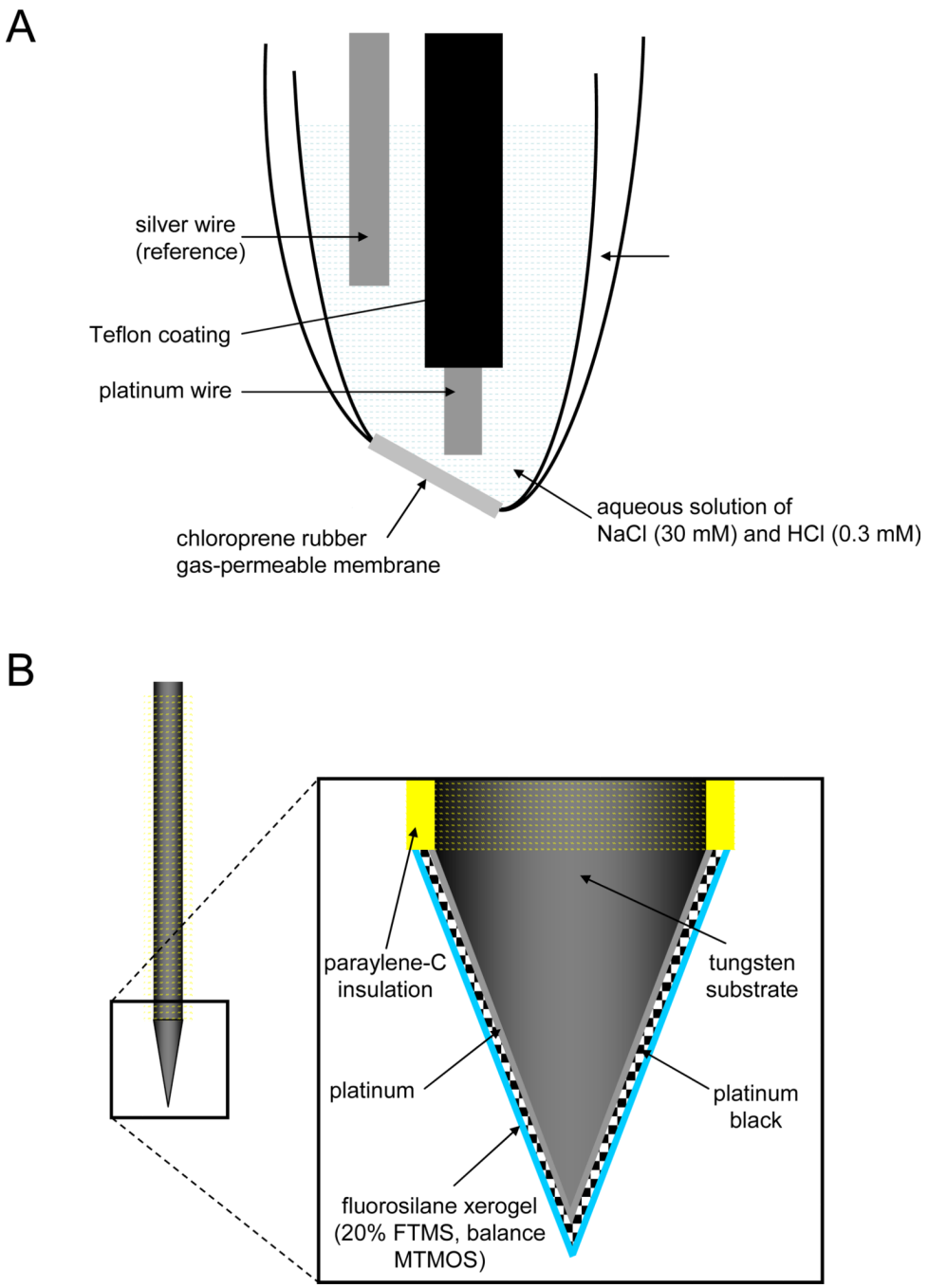

Figure 3.
Diagrams of (A) a Shibuki-style nitric oxide (NO) sensor and (B) a fluorosilane xerogel-coated microelectrode-based electrochemical NO sensor. Note: diagrams not to scale. External reference electrode is not depicted in (B).

Table 1

Summary of nitric oxide (NO) detection techniques with associated limit of detection and detection range.

Class	Method	Technique	Limit of Detection	Detection Range	Reference
SPECTROSCOPIC					
	Absorbance	Hemoglobin assay	1.3 – 2.8 nM	NR[1]	(22)
		Hemoglobin assay (microdialysis)	7 nM	NR	(29)
		Tt Y140F bacterial heme protein	300 nM	30 μM	(30)
		Cytochrome c-doped xerogel	1 ppm	25 ppm	(31)
		Cu(II) eriochrome cyanine R complex	0.23 ppm	6 ppm	(25)
		Griess assay	0.5 μM	NR	(37)
		Griess assay (flow injection analysis)	50 nM	10 μM	(54)
		Griess assay (micro-gas analysis system)	7 ppb	50 ppm	(55)
	Fluorescence	FNOTC[2]	nM range	5 μM	(58)
		Cu(II) fluorescein complex	5 nM	NR	(60)
		Diaminofluoresceins	5 nM	NR	(63)
		TMDABODIPY[3] with HPLC	20 pM	800 nM	(69)
		Cytochrome c'-based probe	20 μM	1 mM	(73)
		Oregon Green 488 gold colloid probe	20 μM	1 mM	(74)
		Oregon Green-labeled cytochrome c'	8 μM	1 mM	(75)
	Chemiluminescence	ozone-based (solution)	nM – pM range	mM range	(76,77)
		ozone-based (gas)	0.5 ppb	500 ppm	(77)
		luminol-based	100 fM	1 nM	(83)
		luminol (polypropylene hollow fiber membranes)	0.3 ppb	≥90 ppb	(84)
		luminol (fiber optic)	1.3 μM	40 μM	(85)
	EPR	Fe-dithiocarbamate spin trap	6 pmol	NR	(106)
ELECTROCHEMICAL					
	Permselective	Shibuki chloroprene rubber membrane	nM range	3 μM	(116)
		Platinized Pt electrode with PTFE[4] membrane	1 nM	≥350 nM	(132)
		Aminoalkoxysilane membrane	25 nM	15 μM	(115)
		Fluoroalkoxysilane membrane	83 pM	4 μM	(135)
	Electrocatalytic	semi-conducting Ni porphyrin	10 nM	300 μM	(108)

Annu Rev Anal Chem (Palo Alto Calif). Author manuscript; available in PMC 2013 February 04.

Class	Method	Technique	Limit of Detection	Detection Range	Reference
	Other	hemoglobin-based electrode	20 pM	5 μM	(137)
		dual NO / CO sensor	1 nM[5]	μM range[5]	(139)

[1] Not Reported

[2] Fluorescent Nitric Oxide Cheletropic Trap

[3] 1,3,5,7-tetramethyl-8-(3',4'-diaminophenyl)difluoroboradiaza-*s*-indacene

[4] Polytetrafluoroethylene

[5] For NO

Annu Rev Anal Chem (Palo Alto Calif). Author manuscript; available in PMC 2013 February 04.